Sustainable Energy & Fuels
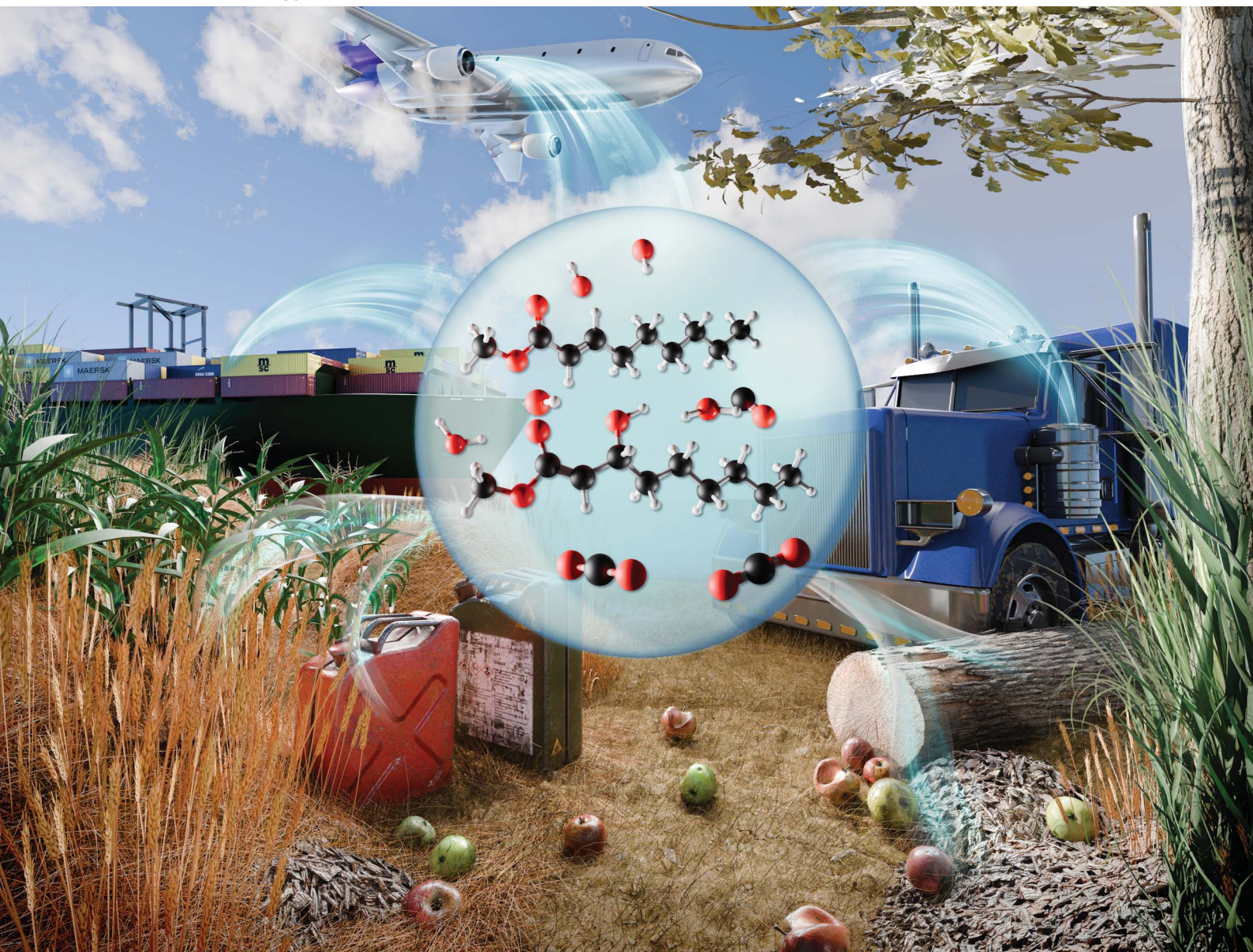
Interdisciplinary research for the development of sustainable energy technologies

rsc.li/sustainable-energy

ROYAL SOCIETY
OF CHEMISTRY

PAPER
Timothy Deehan *et al.*
The influence of Michael acceptors on the structural
reactivity of renewable fuels

PAPER

The influence of Michael acceptors on the structural reactivity of renewable fuels

Timothy Deehan, [ID] * Paul Hellier [ID] and Nicos Ladommatos [ID]

Expanding the use of sustainable fuels in hard to decarbonise transport vehicles utilising heavy-duty engines is urgently required to reduce greenhouse gas emissions from sectors reliant on these engines. As biofuel production turns to alternative sources of biomass with a differing chemical composition to fossil fuel, it is increasingly important to understand how chemical functional groups which may be present in biomass influence the process of combustion. Biofuels are more homogeneous in chemical composition than fossil diesel or gasoline, which are a variety of compounds with a common range of boiling points. As the transport industry progresses in replacing fossil volumes with renewable liquid fuels it also moves towards fuels which are more homogeneous in chemical composition and therefore reactivity. Esters and carbon–carbon double bonds are two common functional groups found in biodiesel and many other classes of bioderived molecules. When adjacent to each other in a specific conformation, they are classed as a Michael acceptor functional group which has a unique reactivity with free radicals separate to either the ester or alkene alone and may play a key role in the low temperature reactions preceding auto-ignition in the combustion process. In this study, the combustion and emissions characteristics of a series of saturated and unsaturated fatty acid esters were tested as single component test fuels, to observe how the inclusion of a Michael acceptor group in esters influences reactivity in a heavy-duty compression ignition engine. Under constant injection duration and timing conditions, it was found that the inclusion of the Michael acceptor in methyl non-2-enoate reduced the duration of ignition delay and increased the IMEP relative to methyl nonanoate and methyl non-3-enoate. Conversely, the inclusion of the Michael acceptor in C_8 and C_{10} ethyl esters resulted in a longer duration of ignition delay and similar observed IMEPs.

Introduction

Recognition of the devastating potential impacts of global climate change has resulted in ambitious targets for the urgent reduction of carbon emissions from the use of fossil fuels. However, industries serviced by large internal combustion engines (ICEs), such as road and marine freight, are considered particularly difficult sectors of the economy to decarbonise.[1] The European Union is pushing for advancement in replacement propulsion systems for ICEs in these sectors; however, electrification has not yet progressed meaningfully in the heavy goods transport sector, and is still not considered a viable technology for the marine sector which instead is incentivised to consider biofuels.[2,3] The incentivisation for expanding biofuel consumption to decarbonise HGVs is lacking in Europe, with the commission redirecting attention to RFNBOs and RCFs.[4] However, outside of Europe, for example in Indonesia, there remains a focus on biofuels, not electrification for the freight and road transport sector.[5]

The development of renewable future fuels (whether RFNBOs or biofuels) presents an opportunity to incorporate molecular structure functionality to improve ignition quality and the efficiency of energy release during combustion, especially as liquid products resulting from biomass conversion or the Fischer–Tropsch process are inherently more homogeneous in chemical structure than fractions of crude oil.[6,7] The focus of research investigating the influence of fuel composition on combustion in heavy-duty engines has so far been dominated by the differences between the major vegetable oils used in biodiesel production,[8] or seeking to replicate the physical properties of fossil diesel.[9]

The pathways through which fuel molecular structure influences combustion in larger compression ignition engines remain an important research topic.[10] The higher compression ratios,[11] greater in-cylinder pressures and slower speeds[12] appreciably alter conditions relative to high-speed light-duty automotive diesel engines and therefore there is a need to explore the effects of fuel composition in the specific context of heavy duty engines.[13,14]

University College London's Mechanical Engineering Department, Roberts Engineering Building, University College London, Torrington Place, London WC1E 7JE, UK. E-mail: timothy.deehan.17@ucl.ac.uk

While fuel development and production often focuses on the realisation of specific physicochemical properties defined by standards such as ASTM 6751,[15] for biofuels differences in molecular structure must be considered to fully explain the performance of certain fuels.[16] For example, dimethyl ether has received widespread attention for use in compression ignition engines owing to its high cetane number and low particulate emissions,[17] despite DME having a lower density and significantly lower boiling point than fossil diesel.[18] In this instance, the ignition quality and potential of DME can instead be attributed to the presence of ether linkages which accelerate the rate of low temperature reaction kinetics towards auto-ignition.[19,20]

Fatty acid methyl esters were quickly adopted as drop-in diesel fuels for their high energy density,[21] miscibility with fossil diesel,[22] and similar physical properties.[23] The chemical difference between biodiesels and fossil diesel is the presence of the ester functional group, and as this is more easily available for fuel radical interactions than the aliphatic hydrocarbon chain, B100 blends can exhibit higher cetane numbers than fossil diesel, resulting in shorter durations of ignition delay.[24]

Further to hydrocarbon fuels, kinetic modelling and shock tube experiments have often focused on esters as these, alongside ethanol, are the most widely available liquid biofuels. Early studies often included methyl crotonate as a simple surrogate for the unsaturated esters found in biodiesel (albeit with a considerably shorter alkyl moiety). Sarathy et al. (2007)[25] and Gaïl et al. (2008)[26] conducted two such studies into the effect of unsaturation on combustion chemistry, and by coincidence of choosing methyl crotonate (methyl but-2-enoate) and methyl butanoate as test fuels for their investigations, the studies also compared the combustion chemistry of saturated esters to α,β-unsaturated esters, a specific functional group which could exhibit unique reactivity compared to a saturated ester.[25] These models improved upon previous schemes where the underlying assumptions had been extrapolated from simple ideal hydrocarbon models, and as further experimental data became available these models were updated to reflect new results. For example, Fisher et al. (2000)[27] presented an early model of reaction kinetics of methyl butanoate and methyl formate combustion, based on existing hydrocarbon models. This was compared against available experimental data, setting the basis of further computational kinetic studies,[28] supported by gas phase kinetic studies[29] and ignition studies in shock tubes.[30]

Sarathy et al. (2007) studied methyl butanoate (MB) and methyl but-2-enoate (M$_2$B) in flame burners and jet stirred reactors, and developed a radical reaction pathway; however, the study did not consider radical addition to the α,β-unsaturated ester (M$_2$B).[25] Gaïl et al. (2008) updated the models for MB and M$_2$B to include additional reaction pathways and potential addition reactions between M$_2$B and H, OH and HO$_2$ radicals were considered; however, the authors focused on discussing the more dominant pathways of fuel consumption.[26]

Kinetic models continued to be updated frequently and dependent on the reaction conditions employed, the radical addition to α,β-unsaturated carbonyls would either be considered a dominant pathway or alternatively unimportant in ester decomposition. This changed when Johnson et al. (2021) and Li

et al. (2022) reviewed these models and focused on including several potential reaction routes which were previously not considered, specifically updating the models to better reflect the radical additions which are available to alkenes.[31,32] Johnson et al.'s main finding was that their new methyl but-2-enoate model came significantly closer to matching experimental observations than the earlier work of Sarathy and Gaïl, which was attributable to the new reactions included. Johnson et al.'s updated model found H or O addition products to M$_2$B to account for 31% of the initial fuel consumption during combustion. Li et al. comparing two structural isomers, methyl acrylate (an α,β-unsaturated ester) and vinyl acetate, in a shock tube found that methyl acrylate exhibited a shorter duration of ignition delay than vinyl acetate and was significantly more active at lower temperatures prior to autoignition. The authors attributed this higher reactivity to hydrogen addition reactions to the double bond consuming the majority of fuel. Liu et al. (2022) conducted a comprehensive investigation into the reaction kinetics of abstraction and addition of methyl hex-3-enoate by H and OH radicals.[33] The authors concluded that H-addition reactions to the C=C double bond are the dominating reaction below 1200 K, with H abstraction dominating above 1250 K. The OH addition to methyl hex-3-enoate was less kinetically favoured than H addition, but remained the dominating reaction over H abstraction below 900 K.[33]

The literature discussed so far on α,β-unsaturated esters has focused on experiments in shock tubes, jet stirred reactors and burners which were used to validate kinetic mechanisms; however, only one previous study investigating the structure of these esters in an actual engine has been reported. Zhang et al. (2009) investigated how premixed ignition reactivity changes with the double bond position in C$_9$ unsaturated esters which included methyl non-2-enoate in the test set, an α,β-unsaturated ester.[34] The experiments were performed in a Cooperative Fuel Research (CFR) engine using a gasoline direct injector in the air intake manifold to provide a homogeneous mixture to the combustion cylinder. The fuels were tested at variable compression ratios, starting at CR 4.43 and increasing until significant high temperature heat release was observed. It was found that the fully saturated methyl nonanoate exhibited significantly higher reactivity in the low temperature region than both methyl nonenoate isomers and that the C$_2$ unsaturated isomer was more reactive than the C$_3$ isomer. Methyl nonanoate exceeded a threshold of 80% of the maximum possible fuel carbon conversion to CO$_2$ at a compression ratio of 7 : 1, whilst methyl non-2-enoate (α,β-unsaturated ester) reached this CO$_2$ value at a CR of 8.5 : 1 and finally methyl non-3-enoate reached this CO$_2$ value at CR 9.5 : 1.[34] The authors concluded that regardless of any additional reaction pathways available, the addition of an alkene in methyl nonanoate reduced its reactivity. However, it is clear that methyl non-2-enoate exhibited appreciably improved combustion relative to methyl non-3-enoate, which the authors attributed to the double bond at the more central C$_3$ position within the alkyl moiety reducing the number of 5 and 6 membered transition rings which can be formed in the low-temperature branching reactions.
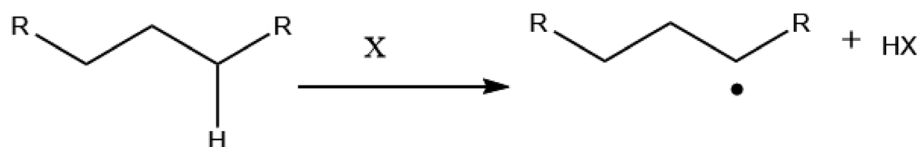
Across all literature investigating unsaturated esters where an α,β-unsaturated ester was used in the comparative set, the authors were unable to fully resolve the behaviour of this fuel relative to structural isomers of the molecule. This is potentially due to the oversight of a unique chemical reactivity exhibited by α,β-unsaturated esters, known as the Michael reaction.[35]

The Michael addition reaction is the nucleophilic addition of a carbanion (or another nucleophile) to an α,β-unsaturated carbonyl compound which was first classed by Arthur Michael in 1897.[36] These two different reagents are commonly referred to as a Michael donor (nucleophile) and Michael acceptor (unsaturated carbonyl). Fig. 1 shows a textbook example of the reaction. The Michael acceptor is a specific functional structure, but the Michael donor can be any negatively charged species and does not require a specific structural motif.[38]

It is important to consider known reactions in the field of organic chemistry as organic radicals are an important species in many synthetic routes and research into fuel chemistry is inherently radical dominated organic chemistry.[39]

The general consensus is that the low temperature reactions which initiate combustion proceed following a hydrogen abstraction from an alkyl chain:[11]
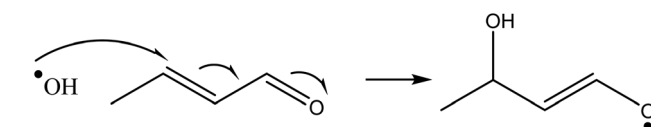

Fig. 2 1,4-Addition of a hydroxyl radical to crotonaldehyde.

Hydrogen abstraction forming water and a carbon centred radical is the only reaction available when a hydroxyl radical encounters cyclohexane, as this is a fully saturated cyclo-alkane. Atkinson *et al.*'s investigation showed that the addition reaction to the alkene portion at the $4'$ position as is typical of a Michael addition reaction had an ~2 to 10 times higher reaction rate constant than hydrogen abstraction of cyclohexane. In the cases of reaction with the 1,4 α,β-unsaturated ketones it was stated with certainty that the reaction proceeds with the addition reaction, but in the case of aldehydes hydrogen abstraction from the aldehyde carbon can also proceed, with the ratio of these two reactions not quantified.[46]

Considering the potential for inclusion of the Michael acceptor functional group in the development of renewable

In the case of oxygenated fuels, the initiated abstraction is often from an adjacent carbon to the oxygenate, owing to the resulting lower bond dissociation energies.[40–42] In the case of unsaturated molecules there is also the potential abstraction from the alkene carbon or additional reactions of other radical species.[43,44]

Atkinson *et al.* (1983) in a study on atmospheric pollutant formation investigated the reaction rates of hydroxyl radicals with 1,4 α,β-unsaturated carbonyl compounds (which can all act as Michael acceptors) and cyclohexane as a comparative molecule.[45] When these compounds react with OH radicals, they can either undergo hydrogen abstraction of any hydrogen present in the molecule forming water and a carbon centred radical, or it can undergo 1,4-addition to the molecule, similar to a Michael donor as shown in Fig. 2.[46]

fuels, one example is that the 1,4 α,β-unsaturated carbonyl could be produced by engineering the fatty acid biosynthesis pathway in microbes.[47,48] This pathway is controlled enzymatically and can potentially be modified such that triglycerides or fatty acids containing the Michael acceptor functional group can be isolated and then converted into suitable biofuels.[49] Many chemical conversions from C_5 and C_6 sugars have been found which result in Michael acceptors, such as the formation of certain acrylates, aspartic acid derivatives, itaconic acid derivatives and levulinic acid derivatives, all of which are considered conventional platform chemicals in lignocellulosic biomass conversion.[50]

This work presents the results of engine experiments in which the combustion and gaseous exhaust emissions of three series of fatty acid ester molecules were investigated. The series
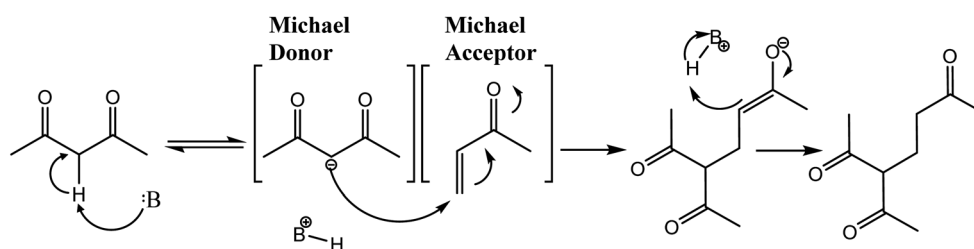
Fig. 1 The Michael addition reaction, a conjugated addition onto an α,β-unsaturated ketone.[37]

were chosen to each include a molecule which contained a Michael acceptor functional group and could be compared to similar molecules which did not contain this group. Relative to previous studies of Michael acceptors, this is the first to utilise a modern direct injection heavy-duty compression ignition engine with a significantly higher compression ratio than previous tests. These experiments were undertaken to test the hypothesis that the inclusion of a double bond on the alpha and beta carbons adjacent to the carbonyl in an ester group, thereby forming a Michael acceptor, may reduce the duration of ignition delay in a slow-speed compression ignition engine.

Heavy-duty engine test facility

All of the combustion experiments presented were performed in a heavy-duty compression ignition engine which was appropriately modified for supplying test fuels to one of the six cylinders while the remaining were supplied with fossil diesel to ensure continuous engine operation. The volume of diesel supplied per cylinder to the back cylinders (two to six) was a much smaller volume than the amount of test fuel supplied to cylinder one, thereby keeping the total engine load below the maximum limit for the water-cooled Schenck Eddy Current Dynamometer W130 which controlled engine speed.

In-cylinder pressure data was read with a Kistler type 6052C pressure transducer installed adjacent to the cylinder one exhaust valves. Injection timing, injection duration and cylinder firing order were controlled by an AVL engine timing unit, timed according to an AND signal from an Turck proximity sensor on the camshaft and a Baumer EIL580-T Optopulse crankshaft encoder with a 0.1 CAD resolution. Experimental data was recorded in a custom LabView environment directly from the timing unit and pressure transducer signals. Pressure data was averaged over 100 continuous combustion cycles during each experiment, and used to calculate the net apparent heat release rate and in-cylinder temperatures exhibited during combustion, using standard heat capacities and values of gamma for in-cylinder gasses presented in Heywood (2018).[51]

Fig. 3 depicts the testing facility, and the divided common rail system and low-volume fuel system used to supply the single component test fuels to the D8k, while Table 1 provides details of the engine specification and operating conditions. The operation of the high-volume test fuel system remains unchanged from that previously reported in detail by Hellier et al. (2011)[52] & Schönborn et al. (2007).[53] Gaseous emissions were measured with a Horiba MEXA 9100 HEGR, incorporating individual instruments to analyse concentrations of each of the CO, CO_2, O_2, NO and NO_x. THC was measured by a Horiba FIA Ov-04 flame ionisation detector.

Test fuels

Seven fatty acid esters were tested as pure components to investigate the effect of including the Michael acceptor structure on compression ignition combustion and emissions. Table 2 provides an overview of these single component fuels with a clear indication of their chemical structure and which are considered potentially able to undergo the Michael reaction.
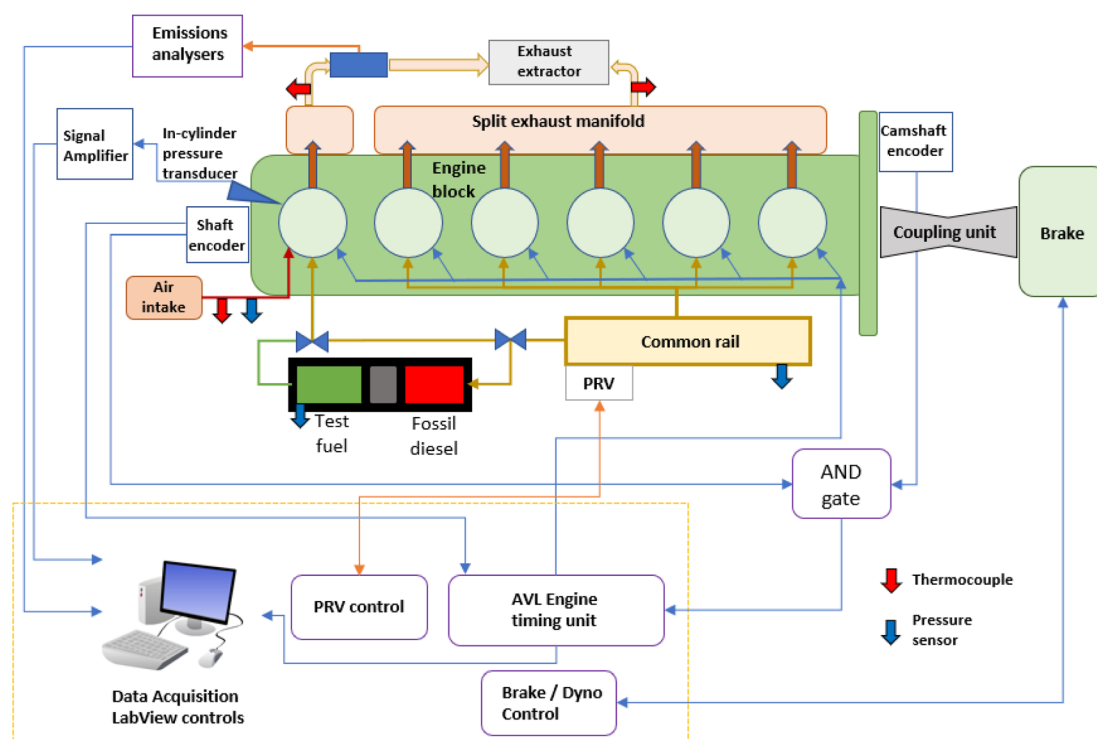

Fig. 3 Overview of the testing facility, showing signal flow between the control components. All thermocouple and pressure sensor signal lines have been omitted for clarity; each of these sends a unidirectional signal to the LabView controls. Shown is the high-volume fuel system which delivered test fuel directly to cylinder 1 only. Abbreviation: pressure relief valve (PRV).

Table 1 Engine Specification

Engine model	Volvo D8k 320
No. of cylinders	6
Displacement	7.7 dm³
Stroke	135 mm
Bore	110 mm
Compression ratio	17.5 : 1
Firing order (where cylinder 1 is that furthest from the flywheel)	1, 4, 2, 6, 3, 5
Engine dimensions $h \times w \times l$ (mm)	1004.06 × 830 × 1252.17
Combustion chamber geometry (mm)	
Piston diameter	108.195 ± 0.012
Con rod length	213.5
Cylinder bore	110
Crank radius	67.5
Clearance volume (mm³)	775.7
Piston bowl geometry	Re-entrant design
Injection pressure	700 ± 5 bar
Shaft encoder	0.1 CAD resolution
Engine speed	820 ± 20 rpm

Three sets of similar molecules were used, two ethyl C_8 esters, three methyl C_9 esters and two ethyl C_{10} esters. As shown in Table 2, each of these sets contains the Michael acceptor equivalent molecule of the fatty acid ester (FAE) single component fuel. The methyl C_9 set further contains methyl non-3-enoate, which is a structural isomer of the Michael acceptor fuel, but the change in double bond position from 2 to 3 prevents it from undergoing the Michael reaction.

These molecules were selected so as to test the hypothesis that inclusion of the Michael acceptor within fatty acid esters would have an appreciable impact on combustion. The differences between the ethyl C_8 and C_{10} fuel sets allowed determination of the effects of fatty acid chain length on Michael acceptor combustion behaviour. The methyl C_9 fuels provide insight into the significance of Michael acceptor structure compared to similar unsaturated esters.

Table 2 shows results of the viscosity and calorific tests of the esters, both of which are key values for the understanding of combustion and were unavailable from previous literature. Due to limited fuel availability, the viscosity and calorific values for methyl nonanoate were not measured.

Experimental procedure

Each of the single component ester fuels, and reference fossil diesel, were tested in the Volvo D8k engine under identical conditions, including a constant engine speed of 820 rpm, constant injection pressure of 700 bar, constant injection timing of 5.3 CAD BTDC and constant injection duration of 6.5 CAD. The injection timing of 5.3 CAD BTDC was chosen as the

Table 2 Overview of the fatty acid ester test fuels, whether or not they are Michael acceptors, skeletal molecular structure and an overview of physical and chemical properties which should be considered during fuel tests of the fatty acid esters and the reference diesel. Purity, boiling point and density data provided by the supplier, Merck. Owing to a limited sample size, the methyl nonanoate viscosity value come from the literature

Fuel (Abbreviations)	Skeletal structure	Michael acceptor?	Boiling point (°C)	Density (g cm⁻³)	Viscosity[a] at 50 °C (Cp)	Gross calorific value[b] (J g⁻¹)
Ethyl octanoate (EtO)		✗	206–208	0.867	1.225 ± 0.015	35 539.3 ± 136.9
Ethyl oct-2-enoate (EtO₂)		✓	222	0.883	1.540 ± 0.030	34 975.3 ± 16.2
Methyl nonanoate (MN)		✗	213	0.875	1.44 (ref. 54)	N/A
Methyl non-2-enoate (MN₂)		✓	215	0.895	1.580 ± 0.020	34 568.7 ± 108.9
Methyl non-3-enoate (MN₃)		✗	213	0.885	1.425 ± 0.025	34 370.7 ± 169.0
Ethyl decanoate (ED)		✗	245	0.865	1.555 ± 0.035	37 230.7 ± 46.0
Ethyl dec-2-enoate (ED₂)		✓	251	0.880	1.890 ± 0.030	36 732.0 ± 30.8
Reference diesel (ref. D)	N/A	✗	189.9–355.5[c]	0.832[c]	2.245 ± 0.035	45 800[c]

[a] Measured using a Brookfield III-Ultra rheometer. [b] Measured using an IKA C1 bomb calorimeter. [c] Technical data for the reference diesel provided by Haltermann Carless.

Table 3 Experimental test conditions and key experimental results for the single component fuel tests in the D8k engine at constant injection timing of 5.3 CAD BTDC, constant injection duration of 6.5 CAD and constant engine speed of 820 ± 20 RPM

Fuel	Michael acceptor?	IMEP (bar)	Ignition delay (CAD)	Duration of combustion (CAD)	APHRR (J deg^{-1})	Timing of APHRR (CAD)	Maximum global calculated in-cylinder temperatures (K)
Ethyl octanoate (EtO)	✗	5.05	6.4	24.9	541.7	363.5	1749.7
Ethyl oct-2-enoate (EtO$_2$)	✓	5.10	8.8	14.8	727.3	367.1	1805.3
Methyl nonanoate (MN)	✗	5.06	6	25.9	417.7	362.7	1706.4
Methyl non-2-enoate (MN$_2$)	✓	5.31	5.9	25.7	450.0	362.6	1776.8
Methyl non-3-enoate (MN$_3$)	✗	5.14	8.4	17.1	800.6	366.4	1826.9
Ethyl decanoate (EtD)	✗	5.59	5.5	27.1	348.2	362	1774.5
Ethyl dec-2-enoate (EtD$_2$)	✓	5.39	7.1	26.1	687.9	364	1790.9
Reference diesel	✗	7.12 ± 0.09	5.2 ± 0.09	32.4	312.2	361.6	1896.5

reference diesel consistently ignited at TDC in preliminary tests verifying the final D8k operating conditions. Table 3 summarises the experimental conditions and key combustion parameters obtained.

Results

In-cylinder pressure and heat release rate

Fig. 4 shows the in-cylinder pressure and apparent heat release rate of methyl nonanoate (MN), the methyl nonenoate isomers

Fig. 4 (a) In-cylinder pressure and (b) apparent heat release rates of methyl nonanoate, methyl nonenoate isomers and reference fossil diesel.

(MN$_2$ & MN$_3$) and reference fossil diesel. Immediately apparent is the significantly longer duration of ignition delay and higher peak heat release rate displayed by MN$_3$ relative to the other test fuels. Also readily visible is that while MN, MN$_2$ and the reference diesel exhibit appreciable heat release in both the premixed and diffusion-controlled combustion phases (albeit less less diffusion-controlled combustion in the case of the esters), that of MN$_3$ is dominated by the premixed burn phase. The longer duration of ignition delay has a direct influence on combustion phasing, allowing for greater air fuel mixing prior to the start of combustion and thus a more combustible mixture available on autoignition, resulting in higher rates of heat release as the fuel is consumed more rapidly.[52]

Visible from the heat release rates (Fig. 4) is that MN exhibited a higher amount of diffusion-controlled combustion relative to the unsaturated esters.

Finally, from Fig. 4 we can observe that moving the double bond from the second to third carbon of the alkyl moiety of the unsaturated methyl esters, from MN$_2$ to MN$_3$, further reduces the extent of diffusion-controlled combustion observed.

Fig. 5 shows the in-cylinder pressure and apparent heat release rate of ethyl octanoate (EtO), ethyl oct-2-enoate (EtO$_2$) and reference fossil diesel. Apparent is the larger period of premixed combustion and lower levels of diffusion-controlled combustion exhibited by both esters compared to reference diesel. It can also be seen that in EtO$_2$ inclusion of a double bond at the 2-position led to a longer ignition delay and higher peak heat release rate relative to the fully saturated EtO.

Fig. 6 shows the in-cylinder pressure and apparent heat release rate of ethyl decanoate (EtD), ethyl dec-2-enoate (EtD$_2$) and reference fossil diesel. Readily apparent is that the majority of heat release occurred during the premixed burn fraction in the case of EtD$_2$. Inclusion of a double bond at the 2-position led to a longer ignition delay and higher peak heat release rate relative to EtD. However, unlike the shorter saturated esters MN and EtO (Fig. 4b and 5b), EtD displayed a similar pattern of heat release to that exhibited by the reference diesel with a larger diffusion-controlled phase (Fig. 4 and 5). This can be attributed to the longer alkyl chain length and subsequently shorter ignition delay allowing less time for the fuel and air to mix before the start of combustion, further leading to a lower premixed burn faction.
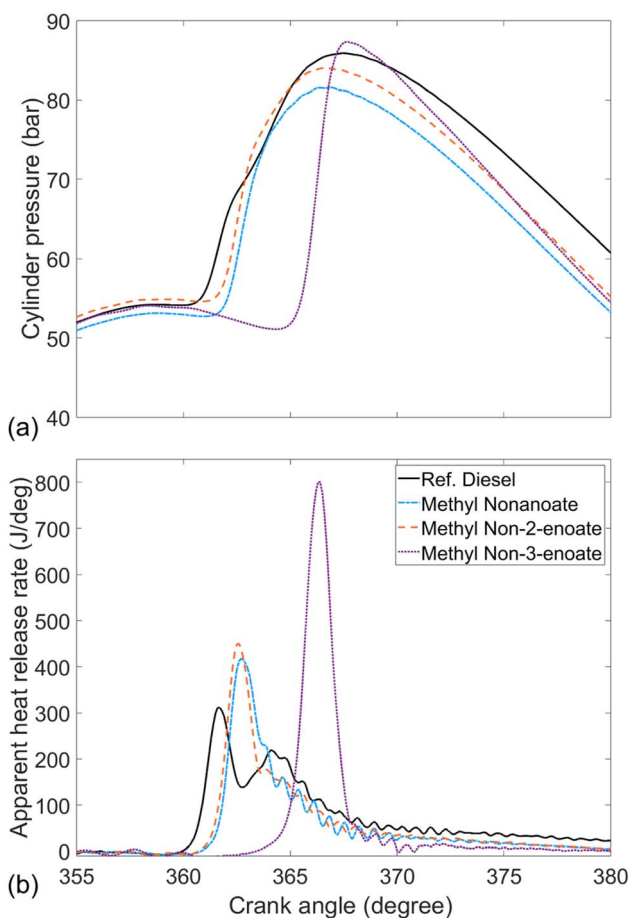
Combustion characteristics

Fig. 7 shows the impact of the Michael acceptor chemical structure on the duration of ignition delay in ethyl C_8, methyl C_9 and ethyl C_{10} saturated and unsaturated esters. In this figure and all subsequent references, ignition delay is defined as the interval between the start of the fuel injection signal supply to the injector control system and the start of combustion as determined from the apparent heat release rate. Additionally, in Fig. 7 and all subsequent figures, the error bars show the standard deviation about the mean of repeat tests of the reference diesel performed alongside the Michael acceptor and other fatty acid ester fuel tests. The ignition delay of MN_3 and EtD_2 showed a slight instance of variability within the 100 consecutive combustion cycles recorded and the coefficient of variance was found to be 0.009 and 0.101 respectively. For the remaining test fuels and reference diesel the coefficient of variance was 0.

Under the constant injection timing conditions, it is apparent from Fig. 7 that all of the fatty acid esters tested exhibited an ignition delay longer than that of the reference diesel.

Fig. 7 also shows a general trend of increasing ignition delay where a carbon-to-carbon double bond is included in the ester alkyl moiety. However, while inclusion of the double bond at the
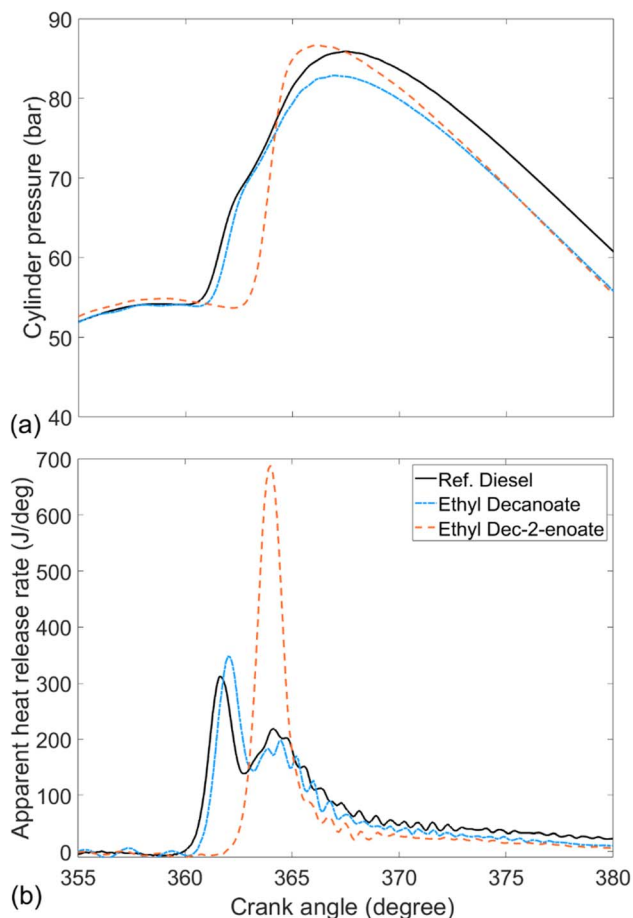
Fig. 6 (a) In-cylinder pressure and (b) apparent heat release rates of ethyl decanoate, ethyl dec-2-enoate and reference fossil diesel.
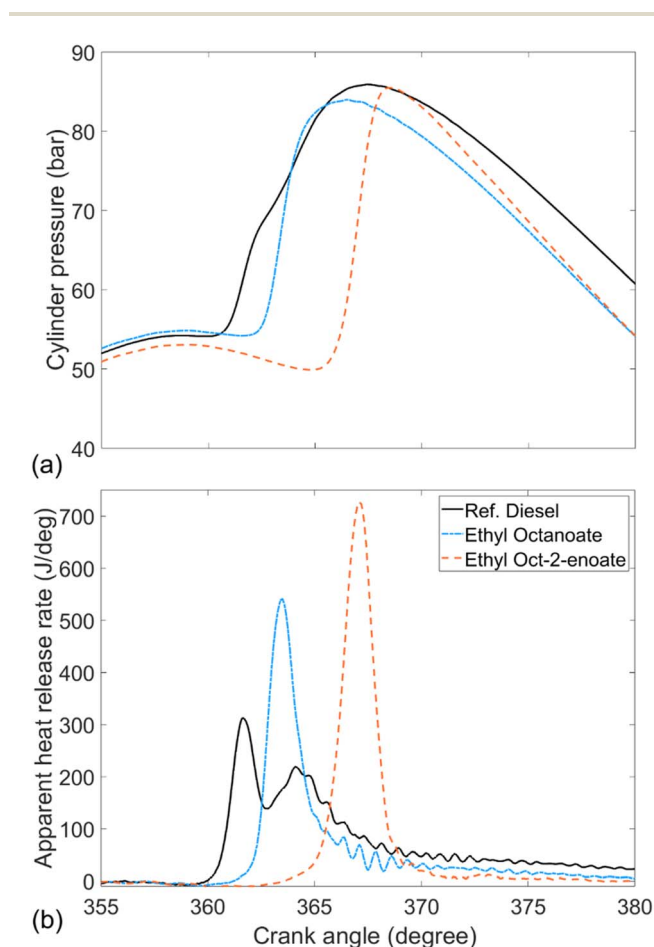
2-position, creating the Michael acceptor chemical structure, increases ignition delay in both EtO_2 and EtD_2, MN_2 displays a reduction in ignition delay relative to the saturated ester of equivalent chain length (MN). Moving the double bond to the 3-position in MN_3 also leads to an increased ignition delay relative to the equivalent Michael acceptor (MN_2).

Fig. 5 (a) In-cylinder pressure and (b) apparent heat release rates of ethyl octanoate, ethyl oct-2-enoate and reference fossil diesel.
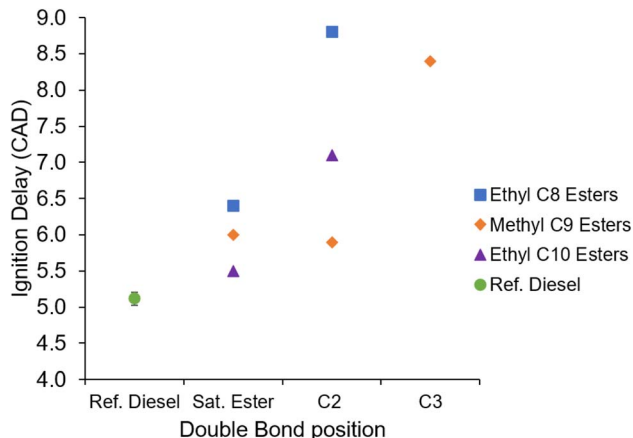
Fig. 7 Ignition delays of the saturated and unsaturated esters, and reference diesel at constant injection timing and duration.

Of the saturated esters, EtD exhibited the shortest duration of ignition delay and EtO the longest; this trend is expected and in agreement with the literature.[55,56] With inclusion of the double bond at the 2-position, this trend is still observed for the ethyl C_8 and C_{10} esters (Fig. 7); however, with the double bond addition the methyl C_9 ester exhibited a shorter ignition delay than the C_{10} ester, an unexpected result as this is contrary to the known trend of hydrocarbon cetane numbers increasing with the number of $-CH_2$ groups in aliphatic chains.[57]

Finally, from Fig. 7 it is clear that the fuel boiling points and viscosities shown in Table 2 had no systematic effect on the wide range of ignition delays observed. MN_2 and MN_3 present with similar values for both physical properties, but the two fuels exhibited ignition delays 2.5 CAD apart. This was larger than the difference in ignition delay of 0.7 CAD exhibited between EtO, which has the lowest boiling point and viscosity, and EtD_2, which has the highest boiling point and viscosity. It is therefore reasonable to assume that the 40 °C difference in boiling point between the two was an insignificant driver of the ignition delays observed.

Fig. 8 shows the IMEP of the saturated and unsaturated esters and reference diesel during combustion with a constant duration of injection. It can be seen in Fig. 8 that all of the ester fuels exhibited an IMEP lower than that of the reference diesel, which is to be expected given the constant injection duration and lower calorific value of the oxygenated fuels (Table 3).

MN and EtO are structural isomers of each other, both having the chemical formula of $C_{10}H_{20}O_2$. These esters both produced approximately 5.1 bar IMEP, whilst the larger EtD produced a 10% increase in IMEP (Fig. 8), attributed to its higher calorific value (Table 3).

Fig. 8 also shows the impact on IMEP of introducing a double to the ester alkyl moiety. Apparent is the slight reduction in IMEP exhibited by EtD_2 relative to EtD, likely due to the lower calorific value of the unsaturated ester (Table 3). Also apparent is the increase in IMEP displayed by MN_2 relative to MN, in contrast to the lower calorific value of MN_2. Of further

note is that the IMEP produced by MN_2 is appreciably higher than that of other esters with the same carbon count; MN, EtO, MN_3 and EtO_2 all exhibit an IMEP value of 5.10 ± 0.05 bar, while an IMEP of 5.31 bar was recorded in the case of MN_2. MN_2 notably has the highest density of the fatty acid esters tested (Table 2), which under the test conditions of constant injection duration and timing may result in a higher mass of fuel entering the combustion chamber relative to the other fuels.[58] However, the relative increase in both viscosity and density between MN and MN_2 is similar to the change in both properties between EtO and Et_2O, and there was no observed difference in IMEP between both fuels. Additionally, the properties of viscosity and density for all seven fatty acid esters were found to be within a tight range relative to the reference fossil diesel (Table 2) and so any changes in IMEP are attributable to improved combustion efficiency.

Fig. 9 shows the peak apparent heat release rate of the saturated and unsaturated esters tested. Is it readily apparent that for all esters, the inclusion of an unsaturated carbon bond results in a higher apparent peak heat release rate (APHRR) relative to their saturated counterparts. In the case of MN_2, the observed increase in APHRR was far less pronounced than those of Et_2O, Et_2D, and MN_3 relative to the saturated esters. The direct influence ignition delay has on the energy release during the premixed combustion phase causes the trends observed in PHRR to closely align with the trends seen in ignition delay, previously shown in Fig. 7. The higher APHRR of MN_2 is also noteworthy as, despite exhibiting a shorter duration of ignition delay relative to MN, it exhibited a higher APHRR which is counterintuitive to the well-established relationship between increasing the duration of ignition delay and observing higher APHRRs.[51,59,60]

Fig. 10a and b show the calculated maximum in-cylinder global temperature and time at which it occurs respectively for the fatty acid esters tested and reference diesel. It can be seen in Fig. 10 that the maximum average cylinder temperature increases for the fatty acid esters with the inclusion of the
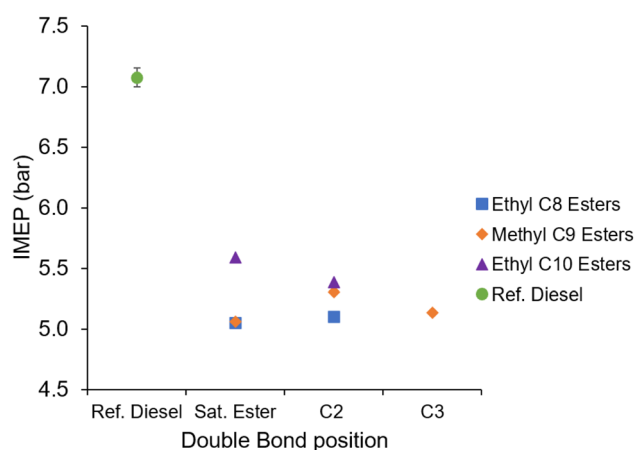

Fig. 8 Indicated mean effective pressure (IMEP) of the saturated and unsaturated esters, and reference diesel at constant injection timing and duration.
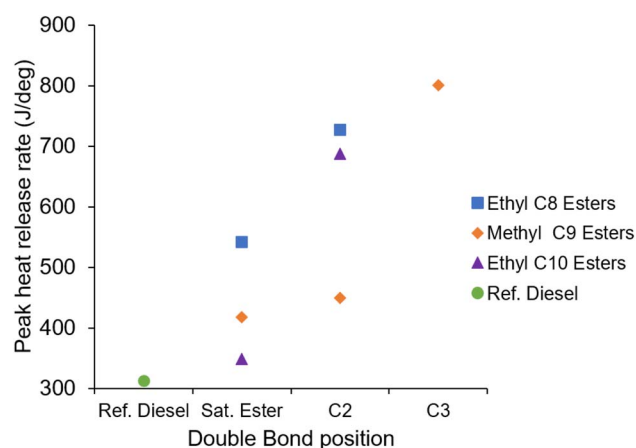

Fig. 9 Peak apparent heat release rate of the saturated and unsaturated esters, and reference diesel at constant injection timing and duration. Error bars are plotted, but are visually insignificant owing to the low variation in reference diesel tests.
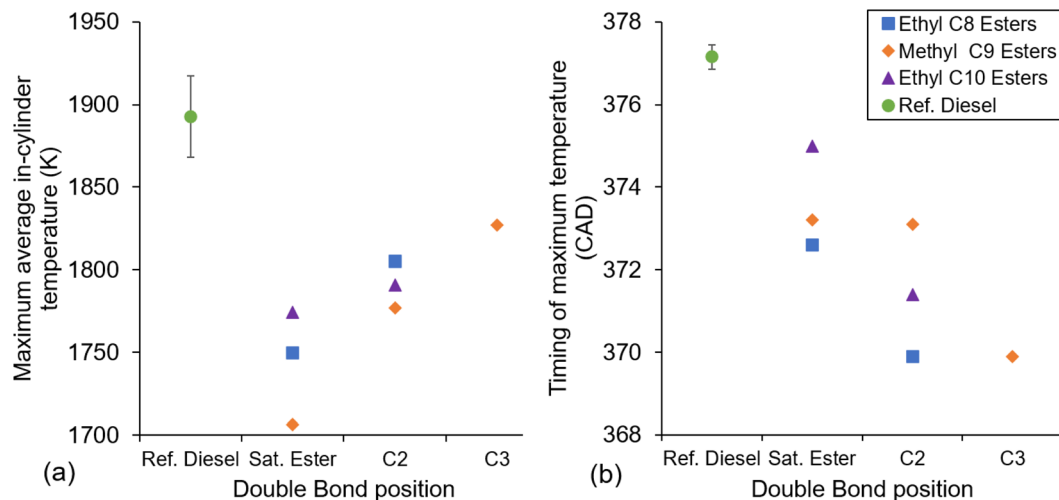
Fig. 10 Maximum average cylinder temperature (a) and timing of maximum temperature (b) of the saturated and unsaturated esters, and reference diesel at constant injection timing and duration.

double bond and increases further as this double bond is moved from the 2-position to 3-position in methyl C_9 esters. Furthermore, the timing of the maximum in-cylinder temperature occurs earlier in the fatty acid esters with the inclusion of the double bond and earlier still as the double bond moves from the 2-position to the 3-position in the methyl C_9 esters. Also apparent in Fig. 10a and b is that the reference diesel reached a significantly higher average temperature and reaches this temperature at a later stage in combustion than the fatty acid esters. This can be attributed to the smaller premixed burn fraction of combustion and larger mixing-controlled phase than the ester fuels (Fig. 4–6).

Fig. 10b shows a reverse trend in timing of maximum temperature to that observed in the duration of ignition delay shown in Fig. 7 and to the level of PHRR shown in Fig. 9. As discussed in the context of Fig. 9, a longer ignition delay resulted in a higher PHRR, which in turn would be expected to lead to an earlier timing of the maximum average in-cylinder temperature.[61,62]

Two exceptions to trends within the fatty acid esters should be noted; the first is that the inclusion of the double bond at the 2-position reverses the relative order of the ethyl esters when considering the calculated maximum in-cylinder temperatures (Fig. 10). The fully saturated decanoate ester, EtD, exhibits a higher maximum average in-cylinder temperature than EtO; however, following the addition of the unsaturated double bond Et_2D instead displays a lower maximum temperature than with Et_2O. For both the saturated and C_2 unsaturated esters, MN and MN_2 exhibit lower maximum temperatures relative to the ethyl esters.

The second notable exception is that the methyl esters do not follow the trend of an earlier maximum average in-cylinder temperature with the unsaturated ester at the 2-position; instead, MN and MN_2 reach their maximum average in-cylinder temperature at almost the same time (± 0.1 CAD).

Fig. 11 shows the duration of combustion exhibited by the ethyl C_8, ethyl C_{10}, and methyl C_9 esters and the reference

diesel. The initial trend to note is that inclusion of a double bond at the 2-position significantly shortened the duration of combustion in Et_2O relative to EtO, whilst MN_2 and EtD_2 remain close to their saturated counterparts. Moving the double bond to the 3-position further leads to a significantly reduced duration of combustion in MN_3. It can further be seen that the three saturated esters exhibit a similar duration of combustion and finally it can be seen that all the ester test fuels exhibit a shorter duration of combustion than the reference diesel.

Previously shown in Fig. 7 was the long ignition delay of MN_3 and EtO_2 with both autoigniting 2.4 CAD after the respective saturated esters. A long duration of ignition delay allows for more of the air and fuel to be well mixed prior to autoignition. Premixed combustion has a short duration and, therefore, the overall combustion period reduces as the amount of premixed combustion increases.[61,63]
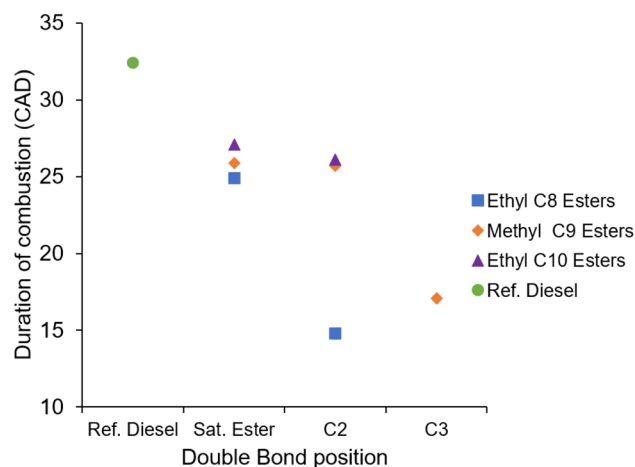

Fig. 11 Calculated duration of combustion of the saturated and unsaturated esters, and reference diesel at constant injection timing and duration. Error bars are plotted, but are visually insignificant owing to the low variation in reference diesel tests.

Exhaust emissions

Fig. 12 shows the measured NO_x emissions during combustion of the three groups of fatty acid esters and reference diesel. Readily apparent is that the NO_x emissions of EtO_2 and MN_3 are significantly higher than those of the other esters and of the reference diesel. This is to an extent an unexpected result, as NO_x emissions would typically correlate with IMEP, and MN, MN_3, EtO and EtO_2 all exhibited similar IMEPs, approximately 5.1 ± 0.1 bar (Table 2 and Fig. 8). Fig. 13 shows the calculated in-cylinder temperature curves for the investigated fuels, in which EtO_2 and MN_3 exhibit the sharpest gradient relative to the remaining test fuels. NO_x is produced either by fuel bound nitrogen, by prompt NO_x, or by thermal NO_x. Under the high temperature conditions of ignition compression, it is most likely the NO_x formed is through oxidation of atmospheric nitrogen and thermal in source, requiring in-cylinder temperatures above 1800 K, known as the Zeldovich mechanism.[64] As shown in Fig. 13, the calculated in-cylinder global temperatures for the reference diesel, EtO_2 and MN_3 surpass this threshold of 1800 K, and as the remaining fuels all surpass 1600 K, it is likely hotspots within the cylinder formed at suitable temperatures for thermal NO_x production.[65]

NO_x production relies on the residence time and stoichiometry of the hot gaseous products of combustion. NO_x production is highly time dependent and the thermochemical kinetics 'freeze' during the expansion stroke when the in-cylinder temperature and pressure decrease.[65]

The longer duration of combustion (Fig. 11) exhibited by the reference diesel, large mixing-controlled burn phase (Fig. 4–6) and higher in-cylinder temperatures (Fig. 13) relative to the esters therefore accounts for the higher NO_x emitted by the reference diesel in comparison to the ester fuels except EtO_2 and MN_3.[65,66]

The significantly higher NO_x emissions of EtO_2 and MN_3 (Fig. 12) can instead be attributed to these two esters exhibiting the longest durations of ignition delay (Fig. 7) which allowed for greater air fuel mixing prior to autoignition. With most of the fuel well-mixed prior to autoignition, the premixed burn phase
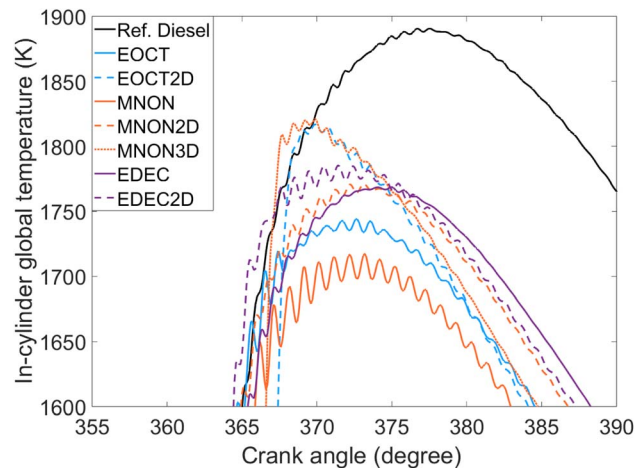

Fig. 13 Calculated in-cylinder global temperatures near TDC of the saturated and unsaturated esters, and reference diesel at constant injection timing and duration.

dominated the combustion process and led to a shorter duration of combustion relative to the other test fuels (Fig. 11). Reaching a higher maximum in-cylinder temperature and completing combustion faster than the ester fuels allows more time for the hot gaseous combustion products to remain at high pressure prior to freezing of NO_x kinetics.[67]

Fig. 14 shows the unburnt hydrocarbon emissions of the fatty acid esters and reference diesel. Apparent are the high levels of THC emitted by EtO_2 and MN_3, which is attributable to the long ignition delay and large premixed burn phase of both esters. A long ignition delay allows for greater air fuel mixing, over-diluting the fuel spray fringe, and creating areas in the chamber which are too lean to auto-ignite or support a self-propagating flame, increasing the amount of unreacted and partially reacted fuel.[68]

Also apparent is the effect of including a double bond in the alkyl chain which resulted in higher observed THC emissions
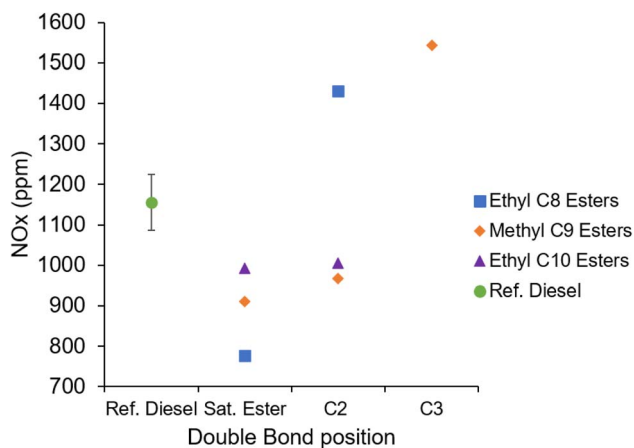

Fig. 12 Exhaust gas NO_x emissions of the saturated and unsaturated esters, and reference diesel at constant injection timing and duration.
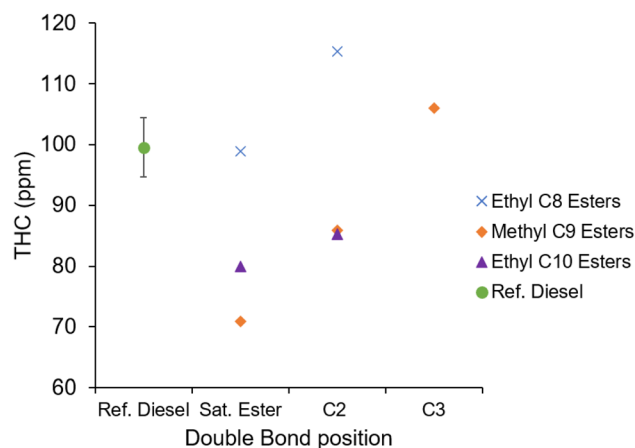

Fig. 14 Exhaust gas unburnt hydrocarbon emissions of the saturated and unsaturated esters, and reference diesel at constant injection timing and duration.

for each of these esters; this is in agreement with higher THC emissions observed from esters with increased olefinic content or a longer duration of ignition delay which both can increase the amount of unreacted fuel.[62,69] Higher THC emissions were also measured from MN_2 relative to MN, despite MN_2 not exhibiting a longer duration of ignition delay (Fig. 7).

Fig. 15 shows the CO emissions of the fatty acid esters and reference diesel. Apparent is the significantly higher emissions of EtO_2 and MN_3, both of which also exhibited increased unburnt hydrocarbon emissions (Fig. 14). As discussed previously, the long ignition delay can lead to areas of air fuel mixture which are too lean to support a self-propagating flame. As with THC emissions, the inclusion of a double bond in the ethyl C_8, ethyl C_{10} and methyl C_9 esters led to increased CO emissions. Also apparent is the lower CO emitted by the reference diesel relative to the esters.

Fig. 16 shows the CO_2 emissions of the ethyl octanoate, ethyl decanoate, and methyl nonanoate esters and reference diesel. Apparent is the lower CO_2 emitted by the esters investigated relative to the reference diesel. All of the test fuels were injected for the same duration (Table 3), therefore the lower CO_2 produced by the esters can be attributed to the lower carbon content by mass resulting from the esters' oxygen content. By molecular weight, the reference fossil diesel has a carbon content of 86.7%, while the carbon content of the esters is approximately 70%, e.g. EtO and MN contain 69.7% and EtD_2 contains 72.7% carbon. The esters therefore contain 16–20% less carbon by mass, which closely aligns with the observation of the esters emitting 18–24% less CO_2.

Impact of the Michael acceptor group on combustion

It is clear from the results discussed in Sections 2.1 to 2.3 that MN_2, a Michael acceptor molecule, exhibits similar combustion phasing (Fig. 4) and levels of exhaust emission species to its saturated analogue, MN. In particular, it has a slightly reduced
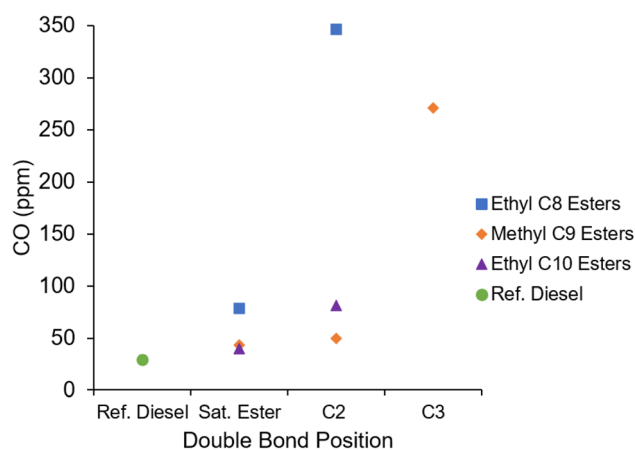
Fig. 15 Exhaust gas CO emissions of the saturated and unsaturated esters, and reference diesel at constant injection timing and duration. Error bars are plotted, but are visually insignificant owing to the low variation in reference diesel tests.
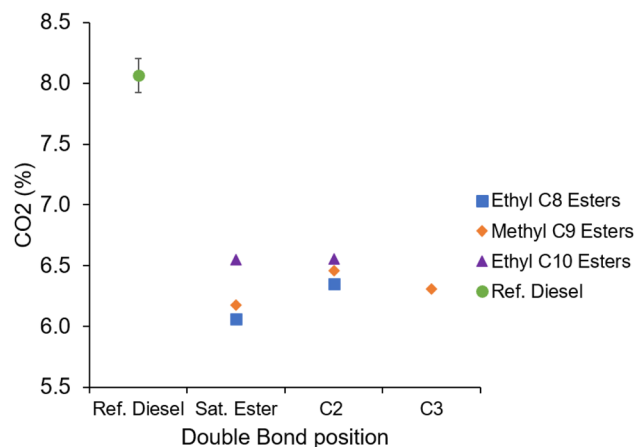
Fig. 16 Exhaust gas CO_2 emissions of the saturated and unsaturated esters, and reference diesel at constant injection timing and duration.

ignition delay (Fig. 7), which correlates with the expectation of radical addition to the double bond outpacing H-abstraction. To further investigate the unique potential of the Michael acceptor functional group within target fuel molecules, a structural isomer of MN_2 was also investigated, MN_3, which is unable to undergo Michael addition. As a single component fuel MN_3 exhibits a significantly longer ignition delay than MN_2, which supports the hypothesis that radical addition to the Michael acceptor in MN_2 is taking place and is important during low temperature kinetics.

Previous work by Zhang et al.[34] investigated the ratio between the low temperature and high temperature heat release for the same methyl C_9 esters investigated within this work. The test fuels were tested in a CFR engine, at increasing compression ratios until significant high temperature heat release was observed, starting at a CR of 4.43 up to a CR of 9.5. They found that MN was far more reactive than MN_2 in the low temperature region. In the work presented here, MN and MN_2 are observed to exhibit similar heat release rates (Fig. 4) and MN_2 exhibits a shorter ignition delay than MN (Fig. 7) indicating higher reactivity. These results observed in the D8k engine can be attributed to the significantly different experimental set up, and higher compression ratio of 17.5, which is more applicable to current engine designs, indicating that the Michael acceptor radical addition route is important to consider in practical diesel engines.

Also clear from the engine tests is that the ethyl C_8 and C_{10} ester test fuels do not follow the same trend with structure as seen in the methyl C_9 esters. In both cases the Michael acceptor molecules EtO_2 and EtD_2 do not exhibit clear similarities relative to the equivalent structural esters as shown between MN and MN_2. Of particular note is that EtO and MN are structural isomers, as are EtO_2 and MN_2, therefore differences observed in combustion characteristics must result from structural isomerism. It is suggested that this difference in reactivity can be attributed to a unimolecular decomposition reaction unique to fatty acid esters with alcohol moieties longer than one carbon. Shown in Fig. 17, this reaction has a low activation energy. Studies by Li et al.[70] and Bennadji et al.[29] have shown that during
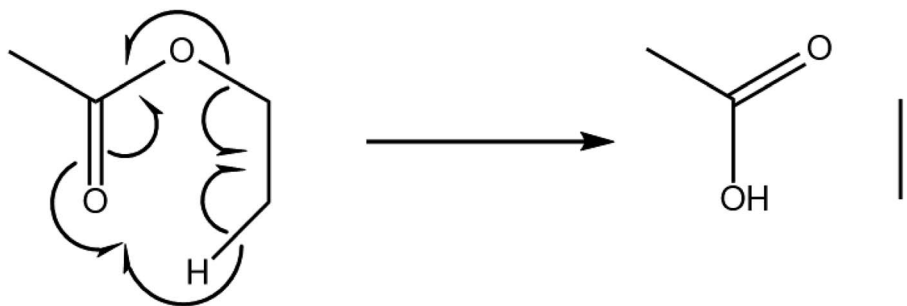
Fig. 17 Ethyl ester undergoing unimolecular decomposition forming a free fatty acid and ethylene.

the combustion of fatty acid ethyl esters, 98% of fuel molecule decomposition is initiated by this reaction.

In the case of the unsaturated ethyl esters, it is expected that they will undergo unimolecular decomposition before any potential Michael addition can occur, as intramolecular reactions generally occur faster than intermolecular reactions. Following unimolecular decomposition, the remaining molecule is an unsaturated carboxylic acid. The carboxylic acid group is significantly less electron withdrawing than an ester group and reduces the reactivity of the unsaturated carbonyl, making the Michael reaction unlikely to occur.[71]

Further to the lower Michael acceptor reactivity, Namysl et al.[72] have shown that H-abstraction in carboxylic acids preferably proceeds at the C_2 position, which in an alpha beta unsaturated carboxylic acid comprises the unsaturated hydrogens which have a higher bond dissociation enthalpy than saturated positions. As an unsaturated carboxylic acid, oct-2-enoic acid would now be expected to exhibit poor combustion.[57]

As with EtO$_2$, the breakdown of EtD$_2$ will initiate via the unimolecular decomposition reaction. In the observed rates of heat release and exhaust emissions EtD$_2$ compared to EtD exhibits poorer performance, with a longer ignition delay, higher PHRR, higher CO and lower IMEP than its saturated counterpart. However, the differences observed between EtD and EtD$_2$ are not as significant as with EtO and EtO$_2$, which can be attributed to the longer carbon chain in the fatty acid moiety of the fatty acid ester. Following unimolecular decomposition EtD$_2$ produces dec-2-enoic acid which allows an increased number of six- or seven-member transition state rings to form relative to oct-2-enoic acid. These transition state rings are a key feature of the low temperature reactions leading to autoignition and their ability to form directly correlates with fuel performance. Increasing alkyl chain length is known to reduce ignition delay, so it is expected that the unsaturated carboxylic acid with a longer alkyl chain would ignite more easily despite the poor reactivity of carboxylic acids.[57,73]

Conclusions

This study investigated the potential differences in combustion caused by the presence of α,β-unsaturated carbonyls (Michael acceptors) within an ester fuel as this chemical structure could provide a unique reaction pathway and shorten the ignition delay.

● In methyl nonanoate inclusion of an alpha beta unsaturated carbon bond, a Michael acceptor, to form methyl non-2-enoate leads to a reduced ignition delay and higher IMEP relative to methyl nonanoate. This agrees with the proposed hypothesis that structures which facilitate radical addition to fuel molecules could reduce ignition delay.

● Movement of the double bond to form methyl non-3-enote from methyl non-2-enote leads to a longer ignition delay, lower IMEP and an increase in undesirable NO_x and CO emissions, indicating that the Michael acceptor present in methyl non-2-enote improved low temperature reactivity relative to unsaturated esters without Michael acceptor reactivity.

● In ethyl octanoate inclusion of an alpha beta unsaturated carbon bond to form ethyl oct-2-enoate leads to a significant increase in ignition delay and emissions of NO_x and CO. Likewise, the inclusion of the alpha beta unsaturated carbon bond in ethyl decanoate to form ethyl dec-2-enoate led to a longer ignition delay and increased pollutant emissions, but to a lesser extent than observed for ethyl octanoate esters.

● The increased ignition delay and poorer performance as a single component fuel of the ethyl ester Michael acceptors can be attributed to the rapid decomposition of the fuel from an unsaturated ester to a less reactive unsaturated carboxylic acid which is unable to undergo Michael acceptor reactions.

In this study of Michael acceptor fuel reactivity, it has been demonstrated clearly that minor changes in chemical structure can result in significant changes in fuel reactivity and combustion profiles in heavy-duty compression ignition engines. Such internal combustion engines as the D8k, or larger, will continue to service the road freight and marine sector for the foreseeable future, necessitating a better understanding of fuel molecular structure. This work also demonstrated the potential detailed chemical reactivity when choosing specific features in fuel. This has the potential to aid in the design of biofuels and renewable fuel with improved fuel properties such as higher ignition quality.

A limitation of the work is the small sample size, as the Michael acceptor could not be tested in an additional set of methyl esters. It is likely further ethyl esters would reflect the same result found here, that the unimolecular decomposition will continue to outpace any available radical intermolecular radical reactions. However, by studying the ethyl esters it has been made clear how intramolecular synergies can influence combustion in complex real world fuel molecules.

Abbreviations

AHRR	Apparent heat release rate
ATDC	After top dead centre
BTDC	Before top dead centre
CAD	Crank angle degree
CFR engine	Cooperative fuel research engine
CO	Carbon monoxide
CO_2	Carbon dioxide
CR	Common rail
C-SOC	Constant start of combustion
C_X (X = any number)	The carbon at position 'X' according to IUPAC convention
D8k	Volvo D8k engine
DAQ	Data acquisition
Dyno	Dynamometer
EtD	Ethyl decanoate
EtD_2	Ethyl dec-2-enoate
EtO	Ethyl octanoate
EtO_2	Ethyl oct-2-enoate
FAE	Faty acid ester
FAME	Fatty acid methyl ester
GHG	Greenhouse gas
ID	Ignition delay
IMEP	Indicated mean effective pressure
MN	Methyl nonanoate
MN_2	Methyl non-2-enoate
MN_3	Methyl non-3-enoate
NO	Nitrogen monoxide
NO_2	Nitrogen dioxide
NO_x	Nitrogen oxides
O_2	Oxygen
PHRR	Peak heat release rate
PRV	Pressure relief valve
PS	Pressure sensor
Ref. D	Reference diesel
rpm	Revolutions per minute
SOC	Start of combustion
THC/UHC	Unburnt hydrocarbons

Data availability

Supporting the publication of "The influence of Michael acceptors on the structural reactivity of renewable fuels" with RSC Sustainable Energy & Fuels, the following data has been uploaded and made publicly available with the Open Science Framework: raw in-cylinder pressure data, raw temperature and emissions data, processed temperature and emissions data, and a summary file containing the results from processing the raw in-cylinder pressure data. Data may be cited with the following information: T. Deehan, P. Hellier and N. Ladom-matos, 2024, Open Science Framework data repository, DOI https://doi.org/10.17605/OSF.IO/MUNVS.

Conflicts of interest

There are no conflicts to declare.

References

1 SMMT P. P., *Charging and Refuelling Requirements of the Heavy Goods Vehicle Sector*, 2023.

2 European Commission, *European Commission-Press Release European Green Deal: EU Agrees Stronger Legislation to Accelerate the Rollout of Renewable Energy*, 2023.

3 European Commission, *What Is the European Geen Deal*, Retrieved Oct. 11, 2021 from https://ec.europa.eu/info/strategy/priorities-2019-2024/european-green-deal_en, 2019.

4 The European Commission, *Commission Delegated Regulation (Eu) 2023/1185*, 2023, vol. 1185, pp. 20–33.

5 M. L. Yeoh and C. S. Goh, Hydrotreated vegetable oil production from palm oil mill effluents: Status, opportunities and challenges, *Biofuels, Bioprod. Biorefin.*, 2022, **16**, 1153–1158.

6 M. E. Dry, The Fischer-Tropsch process: 1950–2000, *Catal. Today*, 2002, **71**, 227–241.

7 A. E. Atabani, A. S. Silitonga, H. C. Ong, T. M. I. Mahlia, H. H. Masjuki, I. A. Badruddin, et al., Non-edible vegetable oils: A critical evaluation of oil extraction, fatty acid compositions, biodiesel production, characteristics, engine performance and emissions production, *Renewable Sustainable Energy Rev.*, 2013, **18**, 211–245.

8 H. Baker, R. Cornwell, E. Koehler and J. Patterson, *Review of Low Carbon Technologies for Heavy Goods Vehicles*, Ricardo, 2010, pp. 1–206, DOI: 10.1038/430006a.

9 T. D. Durbin, D. R. Cocker, A. A. Sawant, K. Johnson, J. W. Miller, B. B. Holden, et al., Regulated emissions from biodiesel fuels from on/off-road applications, *Atmos. Environ.*, 2007, **41**, 5647–5658.

10 N. Mizushima, D. Kawano, H. Ishii, Y. Takada and S. Sato, Evaluation of Real-World Emissions from Heavy-Duty Diesel Vehicle Fueled with FAME, HVO and BTL using PEMS, *SAE Tech. Pap.*, 2014, DOI: 10.4271/2014-01-2823.

11 C. K. Westbrook, H. J. Curran, W. J. Pitz, J. F. Griffiths, C. Mohamed and S. K. Wo, The effects of pressure, temperature, and concentration on the reactivity of alkanes: Experiments and modeling in a rapid compression machine, *Symp. Combust.*, 1998, **27**, 371–378.

12 W. T. Lyn, Study of burning rate and nature of combustion in diesel engines, *Symp. Combust.*, 1963, **9**, 1069–1082.

13 P. D. Patel, A. Lakdawala, S. Chourasia and R. N. Patel, Bio fuels for compression ignition engine: A review on engine performance, emission and life cycle analysis, *Renewable Sustainable Energy Rev.*, 2016, **65**, 24–43.

14 P. R. Ganji, R. N. Singh, V. R. K. Raju and S. Srinivasa Rao, Design of piston bowl geometry for better combustion in direct-injection compression ignition engine, *Sadhana Acad. Proc. Eng. Sci.*, 2018, **43**, 1–9.

15 M. E. Baumgardner, T. L. Vaughn, A. Lakshminarayanan, D. Olsen, M. A. Ratcliff, R. L. McCormick, et al., Combustion of Lignocellulosic Biomass Based Oxygenated Components in a Compression Ignition Engine, *Energy Fuels*, 2015, **29**, 7317–7326.

16 F. Jafarihaghighi, M. Ardjmand, M. Salar Hassani, M. Mirzajanzadeh and H. Bahrami, Effect of Fatty Acid

Profiles and Molecular Structures of Nine New Source of Biodiesel on Combustion and Emission, *ACS Omega*, 2020, **5**, 16053–16063.

17 D. Stepanenko and Z. Kneba, DME as alternative fuel for compression ignition engines – a review, *Combust. Engines*, 2019, **177**, 172–179.

18 J. P. Szybist, S. Mclauglin and S. Iyer, *Emission and Performance Benchmarking of a Prototype Dimethy Ether Fueled Heavy-Duty Truck*, Oak Ridge Nation Labaratory, 2014.

19 L. S. Tran, O. Herbinet, Y. Li, J. Wullenkord, M. Zeng, E. Bräuer, et al., Low-temperature gas-phase oxidation of diethyl ether: Fuel reactivity and fuel-specific products, *Proc. Combust. Inst.*, 2019, **37**, 511–519.

20 C. Arcoumanis, C. Bae, R. Crookes and E. Kinoshita, The potential of di-methyl ether (DME) as an alternative fuel for compression-ignition engines: A review, *Fuel*, 2008, **87**, 1014–1030.

21 R. L. McCormick, M. S. Graboski, T. L. Alleman, A. M. Herring and K. S. Tyson, Impact of biodiesel source material and chemical structure on emissions of criteria pollutants from a heavy-duty engine, *Environ. Sci. Technol.*, 2001, **35**, 1742–1747.

22 G. Anastopoulos, Y. Zannikou, S. Stournas and S. Kalligeros, Transesterification of vegetable oils with ethanol and characterization of the key fuel properties of ethyl esters, *Energies*, 2009, **2**, 362–376.

23 S. A. Basha, K. R. Gopal and S. Jebaraj, A review on biodiesel production, combustion, emissions and performance, *Renewable Sustainable Energy Rev.*, 2009, **13**, 1628–1634.

24 A. Schönborn, N. Ladommatos, J. Williams, R. Allan and J. Rogerson, The influence of molecular structure of fatty acid monoalkyl esters on diesel combustion, *Combust. Flame*, 2009, **156**, 1396–1412.

25 S. M. Sarathy, S. Gaïl, S. A. Syed, M. J. Thomson and P. Dagaut, A comparison of saturated and unsaturated C_4 fatty acid methyl esters in an opposed flow diffusion flame and a jet stirred reactor, *Proc. Combust. Inst.*, 2007, **31**, 1015–1022.

26 S. Gaïl, S. M. Sarathy, M. J. Thomson, P. Diévart and P. Dagaut, Experimental and chemical kinetic modeling study of small methyl esters oxidation: Methyl (E)-2-butenoate and methyl butanoate, *Combust. Flame*, 2008, **155**, 635–650.

27 E. M. Fisher, W. J. Pitz, H. J. Curran and C. K. Westbrook, Detailed Chemical Kinetic Mechanisms, *Proc. Combust. Inst.*, 2000, **28**, 1579–1586.

28 S. M. Sarathy, S. Vranckx, K. Yasunaga, M. Mehl, P. Oßwald, W. K. Metcalfe, et al., A comprehensive chemical kinetic combustion model for the four butanol isomers, *Combust. Flame*, 2012, **159**, 2028–2055.

29 H. Bennadji, P. A. Glaude, L. Coniglio and F. Billaud, Experimental and kinetic modeling study of ethyl butanoate oxidation in a laminar tubular plug flow reactor, *Fuel*, 2011, **90**, 3237–3253.

30 L. Coniglio, H. Bennadji, P. A. Glaude, O. Herbinet and F. Billaud, Combustion chemical kinetics of biodiesel and related compounds (methyl and ethyl esters): Experiments

31 P. N. Johnson, M. L. Lavadera, A. A. Konnov and K. Narayanaswamy, Oxidation kinetics of methyl crotonate: A comprehensive modeling and experimental study, *Combust. Flame*, 2021, **229**, 111409.

32 C. Li, Z. Zhang, L. He, M. Ye, H. Ning, Y. Shang, et al., Experimental and kinetic modeling study on the ignition characteristics of methyl acrylate and vinyl acetate: Effect of C[dbnd]C double bond, *Energy*, 2022, **245**, 123257.

33 B. Liu, Z. Zhou, Z. Zhang and H. Ning, Theoretical Study on Abstraction and Addition Reaction Kinetics for a Medium-Size Unsaturated Methyl Ester: Methyl-3-hexenoate + H/OH Radicals, *J. Phys. Chem. A*, 2022, **126**, 9461–9474.

34 Y. Zhang, Y. Yang and A. L. Boehman, Premixed ignition behavior of C_9 fatty acid esters: A motored engine study, *Combust. Flame*, 2009, **156**, 1202–1213.

35 B. E. P. Kohler and H. Potter, The properties of unsaturated sulfur compounds. I. Alpha beta unsaturated sulfones, *J. Am. Chem. Soc.*, 1935, **57**(7), 1316–1321.

36 A. Michael and O. Schulthess, Ueber die Addition von Natriumacetessig- und Natriummalonsäureäthern zu den Aethern ungesättigter Säuren, *J. Prakt. Chem.*, 1892, **45**, 55–63.

37 F. Wu, H. Li, R. Hong and L. Deng, Construction of quaternary stereocenters by efficient and practical conjugate additions to α,β-unsaturated ketones with a chiral organic catalyst, *Angew. Chem., Int. Ed.*, 2006, **45**, 947–950.

38 B. D. Mather, K. Viswanathan, K. M. Miller and T. E. Long, Michael addition reactions in macromolecular design for emerging technologies, *Prog. Polym. Sci.*, 2006, **31**, 487–531.

39 L. Feray, N. Kuznetsov and P. Renaud, Hydrogen Atom Abstraction, *Radicals Org. Synth.*, 2001, 246–278, DOI: **10.1002/9783527618293.ch39**.

40 S. J. Blanksby and G. B. Ellison, Bond dissociation energies of organic molecules, *Acc. Chem. Res.*, 2003, **36**, 255–263.

41 A. Sudholt, L. Cai, J. Heyne, F. M. Haas, H. Pitsch and F. L. Dryer, Ignition characteristics of a bio-derived class of saturated and unsaturated furans for engine applications, *Proc. Combust. Inst.*, 2015, **35**, 2957–2965.

42 X. You, Y. Chi and T. He, Theoretical Analysis of the Effect of C=C Double Bonds on the Low-Temperature Reactivity of Alkenylperoxy Radicals, *J. Phys. Chem. A*, 2016, **120**, 5969–5978.

43 S. Cagnina, A. Nicolle, T. De Bruin, Y. Georgievskii and S. J. Klippenstein, First-Principles Chemical Kinetic Modeling of Methyl trans-3-Hexenoate Epoxidation by HO2, *J. Phys. Chem. A*, 2017, **121**, 1909–1915.

44 C. W. Zhou, Y. Li, U. Burke, C. Banyon, K. P. Somers, S. Ding, et al., An experimental and chemical kinetic modeling study of 1,3-butadiene combustion: Ignition delay time and laminar flame speed measurements, *Combust. Flame*, 2018, **197**, 423–438.

45 R. Atkinson, S. M. Aschmann and J. N. Pitts, Kinetics of the gas-phase reactions of OH radicals with a series of

α,β-unsaturated carbonyls at 299 ± 2 K, *Int. J. Chem. Kinet.*, 1983, **15**, 75–81.

46 R. Atkinson, S. M. Aschmann and J. N. Pitts, Kinetics of the gas-phase reactions of OH radicals with a series of α,β-unsaturated carbonyls at 299 ± 2 K, *Int. J. Chem. Kinet.*, 1983, **15**, 75–81.

47 Z. Shang, Z. Khalil, L. Li, A. A. Salim, M. Quezada, P. Kalansuriya, et al., Roseopurpurins: Chemical Diversity Enhanced by Convergent Biosynthesis and Forward and Reverse Michael Additions, *Org. Lett.*, 2016, **18**, 4340–4343.

48 A. Miyanaga, Michael additions in polyketide biosynthesis, *Nat. Prod. Rep.*, 2019, **36**, 531–547.

49 S. Vollenweider, H. Weber, S. Stolz, A. Chételat and E. E. Farmer, Fatty acid ketodienes and fatty acid ketotrienes: Michael addition acceptors that accumulate in wounded and diseased Arabidopsis leaves, *Plant J.*, 2000, **24**, 467–476.

50 F. H. Isikgor and C. R. Becer, Lignocellulosic biomass: a sustainable platform for the production of bio-based chemicals and polymers, *Polym. Chem.*, 2015, **6**, 4497–4559.

51 J. B. Heywood, Heat-Release-Rate analysis, in *Internal Combustion Engine Fundamentals*, McGraw-Hill Education, 2nd edn, 2018, pp. 858–860.

52 P. Hellier, N. Ladommatos, R. Allan, M. Payne and J. Rogerson, The impact of saturated and unsaturated fuel molecules on diesel combustion and exhaust emissions, *SAE Tech. Pap.*, 2011, **5**, 106–122.

53 A. Schönborn, N. Ladommatos, J. Williams, R. Allan and J. Rogerson, Effects on diesel combustion of the molecular structure of potential synthetic bio-fuel molecules, *SAE Tech. Pap.*, 2007, DOI: 10.4271/2007-24-0125.

54 C. Wedler and J. P. M. Trusler, Review of density and viscosity data of pure fatty acid methyl ester, ethyl ester and butyl ester, *Fuel*, 2023, **339**, 127466.

55 C. K. Westbrook, C. V. Naik, O. Herbinet, W. Pitz, M. Mehl, S. M. Sarathy, et al., Detailed chemical kinetic reaction mechanisms for soy and rapeseed biodiesel fuels, *Combust. Flame*, 2011, **158**, 742–755.

56 B. Yang, C. K. Westbrook, T. A. Cool, N. Hansen and K. Kohse-Höinghaus, The effect of carbon-carbon double bonds on the combustion chemistry of small fatty acid esters, *Z. fur Phys. Chem.*, 2011, **225**, 1293–1314.

57 M. A. Ratcliff, R. L. Mccormick and J. D. Taylor, *Compendium of Experimental Cetane Numbers Compendium of Experimental Cetane Numbers*, 2017.

58 R. L. Mccormick, J. D. Ross and M. S. Graboski, Effect of several oxygenates on regulated emissions from heavy-duty diesel engines, *Environ. Sci. Technol.*, 1997, **31**, 1144–1150.

59 K. Thakkar, S. S. Kachhwaha, P. Kodgire and S. Srinivasan, Combustion investigation of ternary blend mixture of biodiesel/n-butanol/diesel: CI engine performance and

emission control, *Renewable Sustainable Energy Rev.*, 2021, **137**, 110468.

60 M. Talibi, P. Hellier and N. Ladommatos, Impact of increasing methyl branches in aromatic hydrocarbons on diesel engine combustion and emissions, *Fuel*, 2018, **216**, 579–588.

61 J. B. Heywood, Ignition Delay. in *Internal Combustion Engine Fundamentals*, McGraw-Hill Education, 2nd edn, 2018, 916–940.

62 E. Koivisto, N. Ladommatos and M. Gold, The influence of various oxygenated functional groups in carbonyl and ether compounds on compression ignition and exhaust gas emissions, *Fuel*, 2015, **159**, 697–711.

63 J. B. Heywood, Combustion in Compression-Ignition Engines, in *Internal Combustion Engine Fundamentals*, McGraw-Hill Education, 2nd edn, 2018, pp. 836–839.

64 Y. B. Zeldvich, The Oxidation of Nitrogen in Combustion and Explosions, *J. Acta Physicochim.*, 1946, **21**, 577.

65 J. B. Heywood, Nitrogen Oxides, in *Internal Combustion Engine Fundamentals*, McGraw-Hill Education, 2nd edn, 2018, pp. 978–1005.

66 S. K. Hoekman and C. Robbins, Review of the effects of biodiesel on NO_x emissions, *Fuel Process. Technol.*, 2012, **96**, 237–249.

67 Y. Nada, Y. Komatsubara, T. Pham, F. Yoshii and Y. Kidoguchi, Evaluation of NO_x Production Rate in Diesel Combustion Based on Measurement of Time Histories of NO_x Concentrations and Flame Temperature, *SAE Int. J. Engines*, 2014, **8**, 303–313.

68 J. B. Heywood, Hydrocarbon Emissions, in *Internal Combustion Engine Fundamentals*, McGraw-Hill Education, 2nd edn, 2018, pp. 1010–1059.

69 S. Pinzi, P. Rounce, J. M. Herreros, A. Tsolakis and M. Pilar Dorado, The effect of biodiesel fatty acid composition on combustion and diesel engine exhaust emissions, *Fuel*, 2013, **104**, 170–182.

70 W. Li, C. Cao, X. Zhang, Y. Li, J. Yang, J. Zou, et al., Exploring combustion chemistry of ethyl valerate at various pressures: Pyrolysis, laminar burning velocity and kinetic modeling, *Combust. Flame*, 2021, **227**, 27–38.

71 F. E. Critchfield and J. B. Johnson, Determination of Alpha, Beta-Unsaturated Compounds by Reaction with Sodium Sulfite, *Anal. Chem.*, 1956, **28**, 73–75.

72 S. Namysl, M. Pelucchi, O. Herbinet, A. Frassoldati, T. Faravelli and F. Battin-Leclerc, A first evaluation of butanoic and pentanoic acid oxidation kinetics, *Chem. Eng. J.*, 2019, **373**, 973–984.

73 P. Hellier and N. Ladommatos, The influence of biodiesel composition on compression ignition combustion and emissions, *Proc. Inst. Mech. Eng., Part A*, 2015, **229**, 714–726.